Vol. 12: 205–214, 2011
doi: 10.3354/ab00331

AQUATIC BIOLOGY
Aquat Biol

Published online May 19

Temporal kernels of larval connectivity: a generalised random-walk approach

Stephen M. Chiswell*

National Institute of Water and Atmospheric Research, PO Box 14-901, Kilbirnie, Wellington, New Zealand

ABSTRACT: For many sessile subtidal and intertidal organisms, the connection between isolated adult populations occurs through oceanic dispersal of the larval stage. We define the 'temporal kernel' as the normalised frequency histogram of oceanic dispersal times between otherwise isolated populations, and suggest minimum dispersal times are best defined in terms of a percentile of the temporal kernel. Under certain assumptions, larval dispersal in the ocean can be treated as Gaussian-distributed random-walk motion in the presence of a mean flow. If this is so, the dispersal time is analogous to the 'first-passage time' as described by Schrödinger (1915: Phys Z 16:289–295), and the temporal kernels are described by the inverse Gaussian function. Here, solutions for the temporal kernel are derived for such a model. The solutions for the percentiles of the temporal kernel are exact, but solutions for mean and standard deviation values exist only in the limit of large island separation. The exact and approximate solutions are compared for random walks representative of realistic oceans, and the sensitivity of the temporal kernel to uncertainty in the eddy diffusivity is evaluated.

KEY WORDS: Larval dispersal · Connectivity · Modelling · Dispersal times

INTRODUCTION

It is often supposed that many subtidal and intertidal organisms have a planktonic larval phase in order to aid species dispersal (Scheltema 1971, noted that larval dispersal was recognized by Alfred Russel Wallace as far back as 1876). Thus, for many sessile organisms, the connection between isolated adult populations occurs at the larval stage, and, in recent times, there have been many studies of this larval connection (for a comprehensive review of larval connectivity, see Cowen & Sponaugle 2009).

It has been common to use the term 'dispersal' or 'spatial' kernel to refer to the probability density function of the spatial distribution of larvae at a given time after hatching (e.g. Siegel 2003). These spatial kernels can be modelled in various ways, and can be used to define dispersal length scales and/or make estimates of whether populations are 'open' or 'closed'. For example, Rasmussen et al. (2009) use a numerical ocean model to estimate the spatial distribution of larvae and thence of the connection between populations of mytilid mussels along the Southern California–Northern Baja California coastline.

There are times when one is interested in the distribution of the oceanic dispersal times between 2 isolated populations, since there should be more connection when dispersal times are comparable to the larval duration than when they are not. The simplest view of this temporal connectivity is that isolated populations will be connected only if the minimum dispersal time is less than the larval duration. However, because of variability in oceanic velocities, there is a continuous distribution of dispersal times, and, as a consequence, there is no unambiguous 'minimum dispersal time'. Instead, one has to specify a percentile of the distribution of dispersal times to be taken as a proxy for the minimum dispersal time.

Thus, by analogy with the spatial kernel, this article introduces the term 'temporal kernel' to refer to the frequency histogram (i.e. probability density function) of oceanic dispersal times between otherwise isolated populations. The temporal kernel is purely a function of ocean circulation, does not include larval mortality,

*Email: s.chiswell@niwa.cri.nz

and serves to describe the complete distribution of potential larval dispersal times between 2 otherwise isolated populations.

In the present article, we denote the percentile taken to be a proxy for minimum dispersal time as the 'minimum percentile'. The value of the minimum percentile will depend on the degree of connectivity of interest. One can differentiate between 'evolutionary' and 'ecological (or demographic)' connectivity, where the gene flow needed for ecological connectivity may be 'several orders of magnitude larger' than that for evolutionary connectivity (Cowen & Sponaugle 2009). Thus, the minimum percentile for evolutionary connectivity would be expected to be lower than that for ecological connectivity. For example, 3 common connectivity questions relate to whether isolated island populations may eventually speciate (evolutionary connectivity); the spread of invasive species (ecological); and whether separate fish stocks can be managed independently (ecological).

This was the approach taken by Chiswell (2009) in the study of *Cellana strigilis* limpets, which are thought to have a 3 to 10 d larval phase (Creese 1981). Chiswell (2009) found that limpets at some island pairs were considered the same species even though dispersal times were so long that the maximum larval duration was as low as the 10^{-4} percentile of the temporal kernel. Thus, Chiswell (2009) concluded that the minimum percentile for evolutionary connection could be as low as the 10^{-4} percentile. This low value reflects that very low levels of gene flow between populations are sufficient to maintain species—for example, the 'one-migrant-per-generation' rule appears frequently in studies of genetics (e.g. Mills & Allendorf 1996, Mace & Lande 1991), and was attributed to the importance of extremely rare long-distance dispersal events in maintaining genetic homogeneity between islands (e.g. Kinlan et al. 2005).

The minimum percentile for any particular application may be difficult to determine, but is likely to be low (we discuss this in more detail later); thus, in the present article, we discuss temporal kernels in terms of a few general low percentiles of the dispersal kernel.

Temporal kernels can be derived from an individual-based model, where one releases many numerical larvae at a source location into a time-varying ocean velocity field and compiles the histograms of dispersal times to a destination. The time-varying ocean velocity can be derived either from direct observations of the ocean circulation or from a numerical model. However, there are several potential problems when doing so. First, the numerical model or observations may not capture the complete range of variability values in the ocean circulation—for example, due to different phases of El Niño Southern Oscillation (ENSO) or the Pacific decadal oscillation. (For this reason, connectivity simulations are sometimes run for different oceanic conditions, e.g. Treml et al. (2008) ran a connectivity model separately for strong El Niño, strong La Niña and neutral years.) Second, it is often difficult to accumulate enough arrivals to resolve the statistics of the dispersal times. Chiswell (2009) illustrates this with one example in which only 11 out of 5275 released particles arrived at the expected destination, and made the comment that in order to numerically resolve the low percentiles of arrivals, he would have had to run his model with between 250 and 100 000 times more particles, which would be computationally prohibitive.

It thus seems appropriate to consider whether temporal kernels can be determined from statistical considerations alone. Under certain assumptions, the oceanic dispersal problem can be treated as a 1-dimensional advection–diffusion problem, where the ocean physics is described by a mean velocity and a random walk parameterised in terms of oceanic eddy diffusivity (e.g. Okubo 1994). Developing such an approach provides a theoretical framework in which to interpret the results of model studies, and potentially allows one to determine the statistics of dispersal without having to resort to computing numerous ensembles of particle-tracking simulations.

A 1-dimensional random walk, where the ocean velocity has a Gaussian distribution, is analogous to Brownian motion; thus, we suggest that the dispersal time between 2 isolated populations is analogous to the 'first-passage time' for Brownian motion as described by Schrödinger (1915). If so, the temporal kernels are described by the inverse Gaussian function (Folks & Chhikara 1978), and the problem to be solved is to derive the inverse Gaussian solutions of the temporal kernel as a function of mean velocity and eddy diffusivity.

In the present article, we use the solutions for the spatial kernel of a random-walk model, which are analytic, Gaussian and well known (e.g. Largier 2003), to derive solutions for the temporal kernel. We derive exact analytic solutions for the percentiles of the temporal kernel as a function of mean velocity and eddy diffusivity. These percentiles are numerically shown to be equivalent to those of the first-passage time-inverse Gaussian solutions. It would be both convenient and (by analogy with the spatial solutions) appealing to be able to specify the temporal kernel analytically in terms of its distribution parameters (mean and standard deviation). Unfortunately, the inverse Gaussian function has the property that there is no analytic expression that allows one to derive the distribution parameters from the percentiles, so there is no exact solution for these distribution parameters as a function

of ocean statistics. There are, however, analytic solutions for the distribution parameters that are valid only in the limit of large population separation, and so, as described in Supplements 1 & 2 (at www.int-res.com/articles/suppl/b012p205_supp.pdf), we evaluate these approximate solutions against numerically determined exact values for realistic ocean conditions using Monte-Carlo simulations.

Thus, the main aims of the present article are:

(1) to introduce the term 'temporal kernel'

(2) to show that for a Gaussian-distributed random-walk ocean, the temporal kernel can be described by an inverse Gaussian distribution

(3) to derive analytic expressions for the temporal kernel as functions of the ocean statistics, along with their sensitivity to uncertainties in ocean parameters.

This article proceeds as follows. The next section reviews the solutions for the spatial kernel. These solutions are then used to derive solutions for the temporal kernel. We then discuss the practical use of temporal kernels. In practice, the most uncertain ocean parameter is likely to be eddy diffusivity, so we show how the low percentiles are sensitive to these uncertainties in eddy diffusivity. Finally, we discuss the choice of the relevant percentile used to interpret connectivity.

SPATIAL KERNEL

Fig. 1 schematically illustrates the 1-dimensional connectivity problem, showing the spatial and temporal solutions, respectively. The spatial solution refers to the distribution of larvae originating from a source at some given time, t, after hatching. Usually this time would be the larval duration for the species of interest. The temporal solution deals with the distribution of dispersal times between source and destination populations at a fixed separation, D.

We assume the velocity field can be described as a mean flow plus random walk, where the random walk has a Gaussian distribution and is designed to simulate the ocean's mesoscale eddy variability. This mesoscale eddy variability can be regarded as a diffusive process parameterised in terms of eddy diffusivity, K. Thus, the 1-dimensional Lagrangian velocity, u (i.e. the velocity seen by an individual larva), can be described as a Markov 1 random walk (e.g. Rupolo 2007) in the presence of a mean flow:

$$u(t) = u_0 + u'(t) \quad (1)$$

where u_0 is the mean velocity and u' is the random walk. This random walk is specified to be normally distributed, have variance u_1^2 and a Lagrangian decorrelation timescale, T_L. The Lagrangian decorrelation timescale is the integral of the Lagrangian velocity autocorrelation function, and is a measure of the spectrum of the eddy processes that lead to diffusion in the ocean—larger T_L corresponds to a more red spectrum. The eddy diffusivity, K, is the product of Lagrangian decorrelation timescale multiplied by the velocity variance (e.g. Rupolo 2007):

$$K = u_1^2 T_L \quad (2)$$

Thus, the ocean can be statistically represented to the first order by a mean velocity and eddy diffusivity.

The spatial and temporal kernels can be derived using solutions to the classic single-particle dispersion problem (e.g. Babiano et al. 1987). In the single-particle

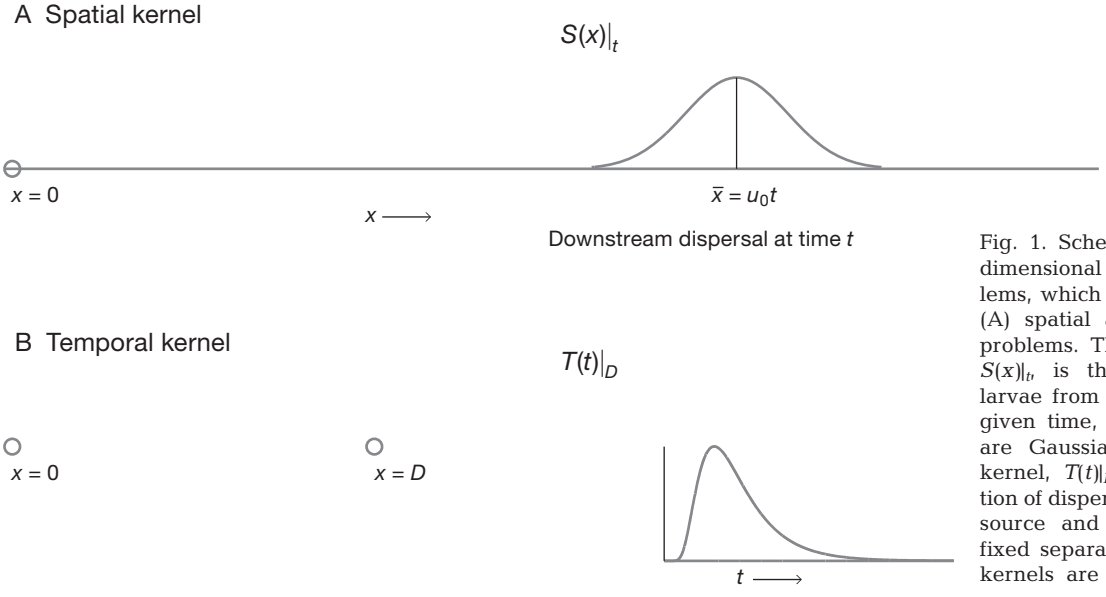

Fig. 1. Schematic showing 1-dimensional connectivity problems, which are referred to as (A) spatial and (B) temporal problems. The spatial kernel, $S(x)|_t$, is the distribution of larvae from a source at some given time, t. Spatial kernels are Gaussian. The temporal kernel, $T(t)|_D$, is the distribution of dispersal times between source and destination at a fixed separation, D. Temporal kernels are inverse Gaussian

problem, one repeatedly releases a single particle at the source at some prescribed time interval. The dispersal statistics are computed from ensemble averages of many releases. Each release is independent (i.e. each particle has no memory of preceding releases), so that the time interval of release should be longer than the decorrelation timescale of the ocean velocities. For example, one might use a numerical model to simulate the release of a single particle from a particular island every month over 100 yr, and use the 1200 resulting trajectories to compute the dispersal statistics.

For single-particle dispersion, the distribution of displacement, x, at a given time, t, i.e. the spatial kernel, $S(x)|_t$, is expected to be Gaussian (Largier 2003, and references therein):

$$S(x)|_t = \frac{1}{\sqrt{2\pi}\sigma_x}\exp\frac{-(x-\bar{x})^2}{2\sigma_x^2} \quad (3)$$

where $\bar{x}$ and σ_x are the means and standard deviations of the displacement. The integral of the spatial kernel is 1 so that the spatial kernel can be regarded as a probability density function. The mean displacement and variance both increase linearly in time:

$$\bar{x} = u_0 t \quad (4)$$

and

$$\sigma_x^2 = 2Kt \quad (5)$$

Thus, Eqs. (4 & 5) completely describe the evolution in time of the spatial kernel for an ocean specified by u_0 and K.

TEMPORAL KERNEL: EXACT SOLUTIONS

The derivation of the temporal kernel at location D can be visualised with reference to Fig. 2, which shows the spatial kernel at 3 different times for an ensemble of single-particle releases flowing past D at mean speed u_0. The 3 times were chosen so that, at time $t = \tau_{16}$, 16% of particles have passed location D, at $t = \tau_{50}$, the ensemble is centred on D and, at time $t = \tau_{84}$, 16% of particles have yet to pass location D. These times are, respectively, the 16th, 50th and 84th percentiles of the temporal kernel. The value of 16% was chosen for this illustration because it is the percentile that occurs 1 standard deviation away from the mean for the Gaussian distribution. At these 3 times, the spatial ensemble is centred at $x = D - \sigma_{16}$, $x = D$ and $x = D + \sigma_{84}$, respectively, where σ_{16} and σ_{16} are the standard deviations at $t = \tau_{16}$ and $t = \tau_{84}$.

The second case shows that the median percentile, τ_{50}, occurs when the spatial ensemble is centred on D, and, from Eq. (4), one immediately obtains an equation for the median percentile of the temporal kernel:

$$\tau_{50} = D/u_0 \quad (6)$$

The first and third cases in Fig. 2 can be generalised for any nth percentile of the temporal kernel by observing that, at $t = \tau_n$, the spatial ensemble is centred at:

$$x = D + g_n\sigma_n \quad (7)$$

where g_n is obtained from the cumulative density function for the Gaussian distribution:

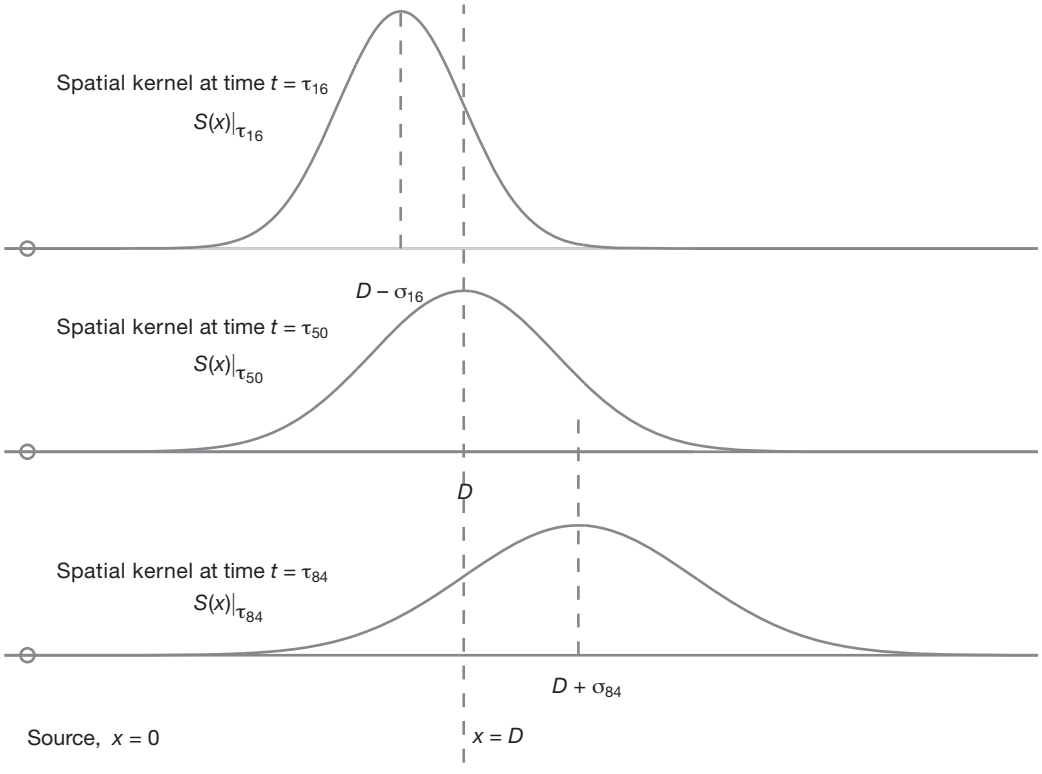

Fig. 2. Schematic showing the advection of a Gaussian-distributed ensemble of particles past location D, at times τ_{16}, τ_{50} and τ_{84}, when 16%, 50% and 84%, respectively, of the particles have passed D. The ensemble is centred at $D - \sigma_{16}$, D and $D + \sigma_{84}$ at these times. Because the spatial kernel expands in time, $\sigma_{16} < \sigma_{84}$, with the result that the temporal kernel is skewed in time

$$g_n = \sqrt{2}\,\mathrm{erf}^{-1}(2n/100 - 1) \quad (8)$$

where erf^{-1} is the inverse error function (i.e. $g_1 = -1$, $g_{50} = 0$, etc.). From Eqs. (4) and (5), one obtains 2 equations for the mean and standard deviation of the spatial ensemble at time $t = \tau_n$:

$$\tau_n = (D - g_n\sigma_n)/u_0 \quad (9)$$

and

$$\sigma_n^2 = 2K\tau_n \quad (10)$$

These equations can be combined to produce an equation for the nth percentile

$$u_0\tau_n + g_n\sqrt{2K\tau_n} - D = 0 \quad (11)$$

Eq. (11) is a quadratic in $\sqrt{\tau_n}$ and can be solved numerically. Because g_n has the property that $g_n = -g_{100-n}$, the 2 roots of the solution give τ_n and τ_{100-n}, so that:

$$\tau_n = \left(\frac{-g_n\sqrt{K} - \sqrt{g_n^2K + 4u_0D}}{2u_0}\right)^2 \quad (12)$$

and

$$\tau_{100-n} = \left(\frac{-g_n\sqrt{K} + \sqrt{g_n^2K + 4u_0D}}{2u_0}\right)^2 \quad (13)$$

An analytic form for the temporal kernel $T(t)|_D$, which produces the percentiles described by Eqs. (12) & (13), can be derived by noting that the first-passage time, as described by Schrödinger (1915) for Brownian motion, is the time taken for a particle to first traverse a distance D, and so is analogous to the dispersal time. This first-passage time distribution is the inverse Gaussian function (Folks & Chhikara 1978):

$$T(t)|_D = \left(\frac{\lambda}{2\pi t^3}\right)^{1/2} \exp\frac{-\lambda(t-\bar{t})^2}{2\bar{t}^2 t} \quad (14)$$

where $\bar{t}$ is the mean dispersal time, and $\lambda = \bar{t}^3/\sigma_t^2$, where σ_t is the standard deviation of dispersal times.

The inverse Gaussian function has the unfortunate property for this work that there is no analytic expression that allows one to derive the distribution parameters ($\bar{t}$ and σ_t) from the percentiles. However, one can compute these values numerically. Fig. 3 illustrates this process for a numerical ocean having $u_0 = 0.05$ m s^{-1}, $K = 3.5 \times 10^3$ m^2 s^{-1} and a separation of 300 km. One starts by choosing a set of percentile values n and computing the respective percentile times, τ_n. Here, we have chosen n to be every 5th percentile between 1 and 96, but added both low and high percentiles to increase resolution at the tails of the distribution. The left-hand panel of the figure shows n plotted as a function of τ_n. The temporal kernel is then obtained by numerically differentiating n with respect to τ_n as shown in the right-hand panel. One can then fit an inverse Gaussian function to this numerical distribution by standard non-linear fitting routines. The right-hand panel shows a fit made using a Levenberg-Marquardt non-linear fitting routine. The mean, $\bar{t}$, and standard deviation, σ_t, of dispersal times for this fit are 88.3 and 65.1 d, respectively.

That the temporal kernels of a Gaussian-distributed velocity ocean are inverse Gaussian can be demonstrated using a Monte-Carlo simulation. Supplement 2 (www.int-res.com/articles/suppl/b012p205_supp.pdf) describes a Monte-Carlo method for generating ensembles of particle trajectories for an ocean having the characteristics specified by Eqs. (1) & (2), and Fig. 4 illustrates simulated temporal kernels for a numerical ocean having $u_0 = 0.05$ m s^{-1} and $K = 3.5 \times 10^3$ m^2 s^{-1}. The panels show histograms of dispersal time derived from the Monte-Carlo simulations for 3 different separations, along with inverse Gaussian fits derived from the method illustrated in Fig. 3. The panels also list the means and standard deviations of dispersal time ($\bar{t}$ and

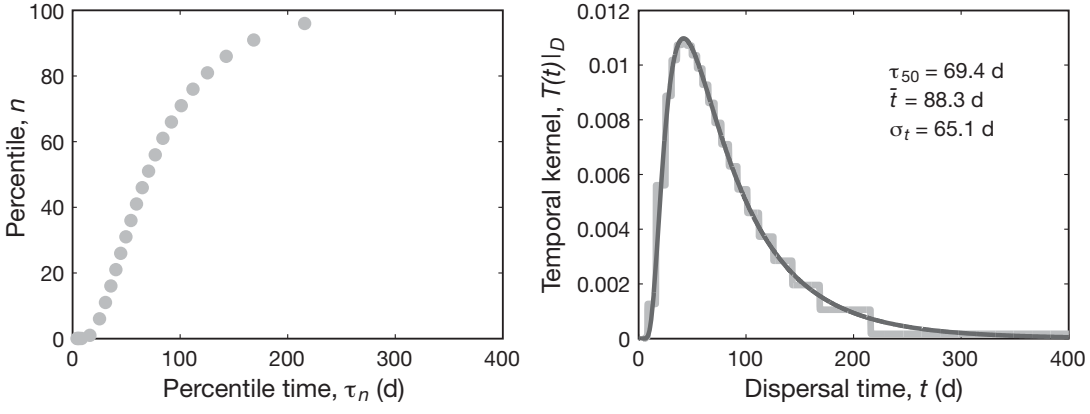

Fig. 3. Schematic showing how to compute the temporal kernel, $T(t)|_D$ from percentile dispersal times, τ_n, calculated according to Eq. (12). The left panel shows the percentiles, n, plotted as a function of τ_n for an ocean where mean velocity, $u_0 = 0.05$ m s^{-1}, eddy diffusivity, $K = 3.5 \times 10^3$ m^2 s^{-1}, and with a separation of 300 km. The right panel shows the numerical derivative of this curve (light grey line). Superimposed is an inverse Gaussian fit made to the numerical derivative, having mean ($\bar{t}$) and standard deviation (σt) in dispersal time as listed (dark grey line)

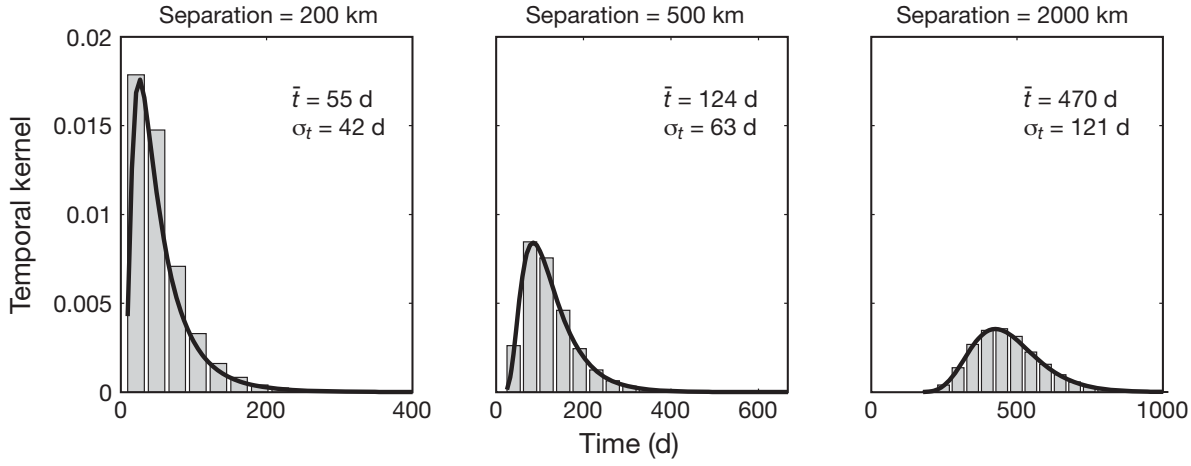

Fig. 4. Temporal kernels from a Monte-Carlo simulation for a numerical ocean where mean velocity, $u_0 = 0.05$ m s^{-1}, and eddy diffusivity, $K = 3.5 \times 10^3$ m^2 s^{-1}. The panels show the simulated temporal kernels (bars) for separations of 200, 500 and 2000 km, respectively. Inverse Gaussian solutions for each kernel are shown (solid lines). Mean ($\bar{t}$) and standard deviation (σ_t) dispersal time for each kernel are as indicated

σ_t) for each simulation. The temporal kernels are positively skewed and well fit by an inverse Gaussian distribution. As the separation increases, the temporal kernels become less skewed and become more Gaussian.

PRACTICAL APPLICATIONS

There are 2 main practical applications of this work. The first application is that it provides a theoretical basis for choosing the inverse Gaussian distribution to fit the histograms of dispersal time derived from individual particle-based simulations. It is often difficult in these simulations to get many particles to arrive at the destination—as in the real world, by far the majority of released larvae never arrive at the destination. Since it is the low percentiles that are usually important when computing connectivity (Chiswell 2009), the low rates of arrivals mean that these low percentiles often cannot be computed directly from the histograms of simulated dispersal times because the tails of the histograms will not be well resolved. In addition, the number of arrivals can vary hugely between different source–destination pairs. Thus, fitting an analytic function to the histograms allows one both to resolve the low-percentile tails of the temporal kernel, and to compare source–destination pairs that have vastly different arrival rates. Fig. 5 illustrates this, where we show the histograms of dispersal time for several island pairs from Chiswell (2009). In the best case (Campbell to Bounty Island), there were 1490 arrivals, but for Bounty to Chatham Islands there were only 32 arrivals. Several island pairs (not all are shown) had about 100 arrivals. By fitting inverse Gaussian distributions to these histograms, one can compute any desired percentile, and the figure shows the first percentile, τ_1, derived from these fits. In 2 cases, τ_1 is less than the shortest simulated dispersal time.

Chiswell (2009) fits log-normal curves to his modelled histograms, and the figure shows these original fits together with the respective estimates of the first percentile of dispersal time. Fortunately, over a large range of likely oceanic conditions, the inverse Gaussian and log-normal distributions are virtually indistinguishable so that the results of Chiswell (2009) are not in jeopardy.

The second application of this work is that one can compute the temporal kernel without performing extensive particle-based simulations. In order to do this, one needs *a priori* estimates of the mean velocity and eddy diffusivity over the dispersal paths, each of these will have some error. The mean velocity can usually be reasonably well determined from climatologies (e.g. obtained from surface drifters; Fratantoni 2001), but eddy diffusivity is more difficult to estimate (e.g. Zhurbas & Oh 2003), and its uncertainty is likely to have the most impact on the calculation. It is thus useful to perform an analysis on the sensitivity of the results to uncertainties in *K*. Here, we illustrate such a sensitivity analysis for 4 hypothetical island pairs representative of those studied by Chiswell (2009). In that study, the island separations ranged from 609 to 1673 km, and the deduced mean velocities between the islands ranged from 0.08 to 0.15 m s^{-1}. Thus, we chose 2 mean velocities (u_0 = 0.05 and 0.15 m s^{-1}) and 2 separations (D = 500 and 1500 km), and computed the temporal kernels as a function of eddy diffusivity for all 4 combinations of u_0 and D. The span in eddy diffusivity was based on estimates of K made using Lagrangian drifter data in the New Zealand region that ranged from 2.6×10^3 to 6.1×10^3 m^2 s^{-1} (Chiswell et al. 2007).

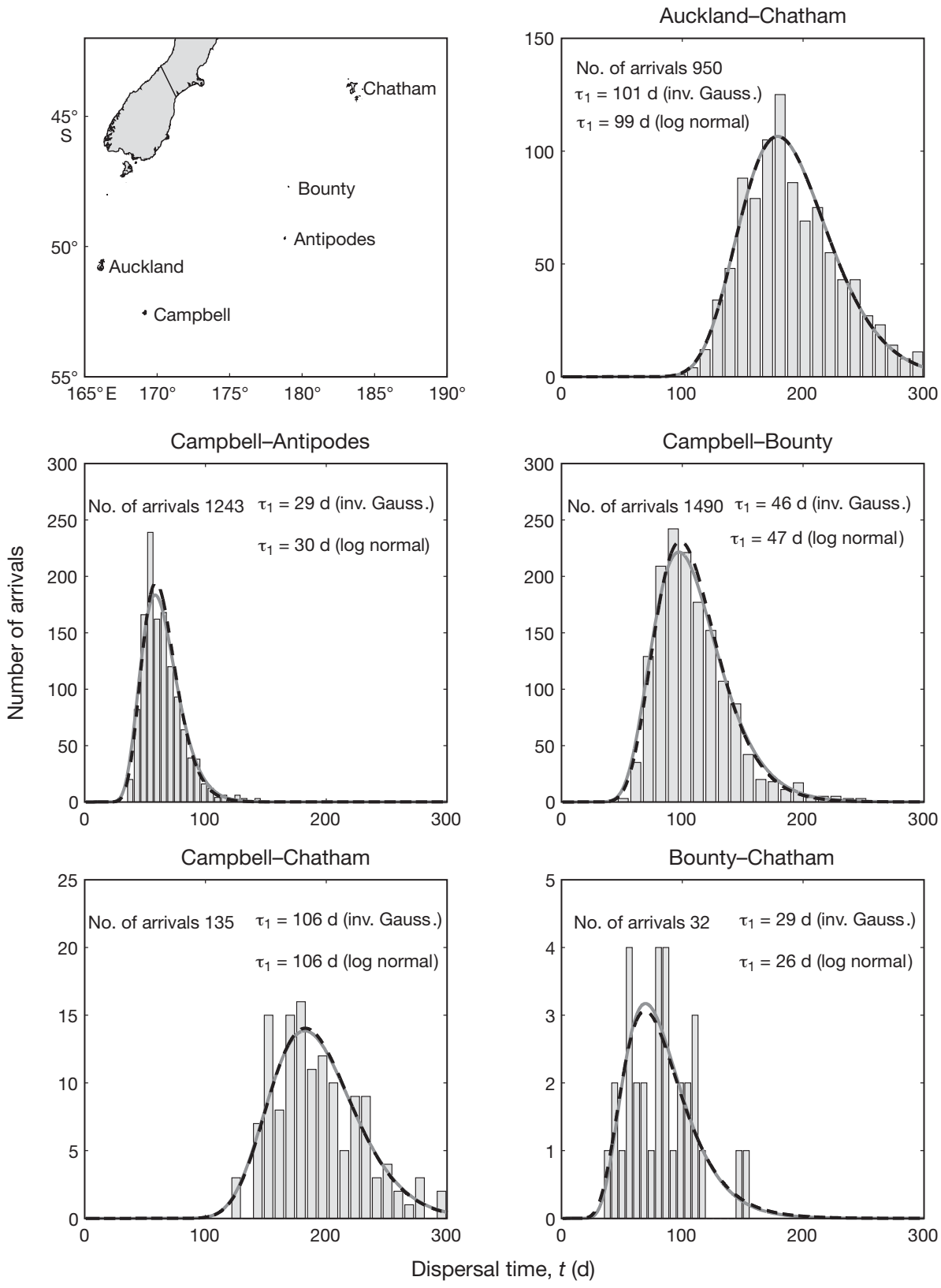

Fig. 5. Histograms of dispersal time for various island pairs from Chiswell (2009), along with inverse Gaussian (solid grey lines) and log-normal (dashed black lines) fits to the histograms. Also shown are the total numbers of arrivals in each histogram, together with first percentiles τ_1 from each fit. Headers indicate the source–destination islands shown in the upper left-hand panel

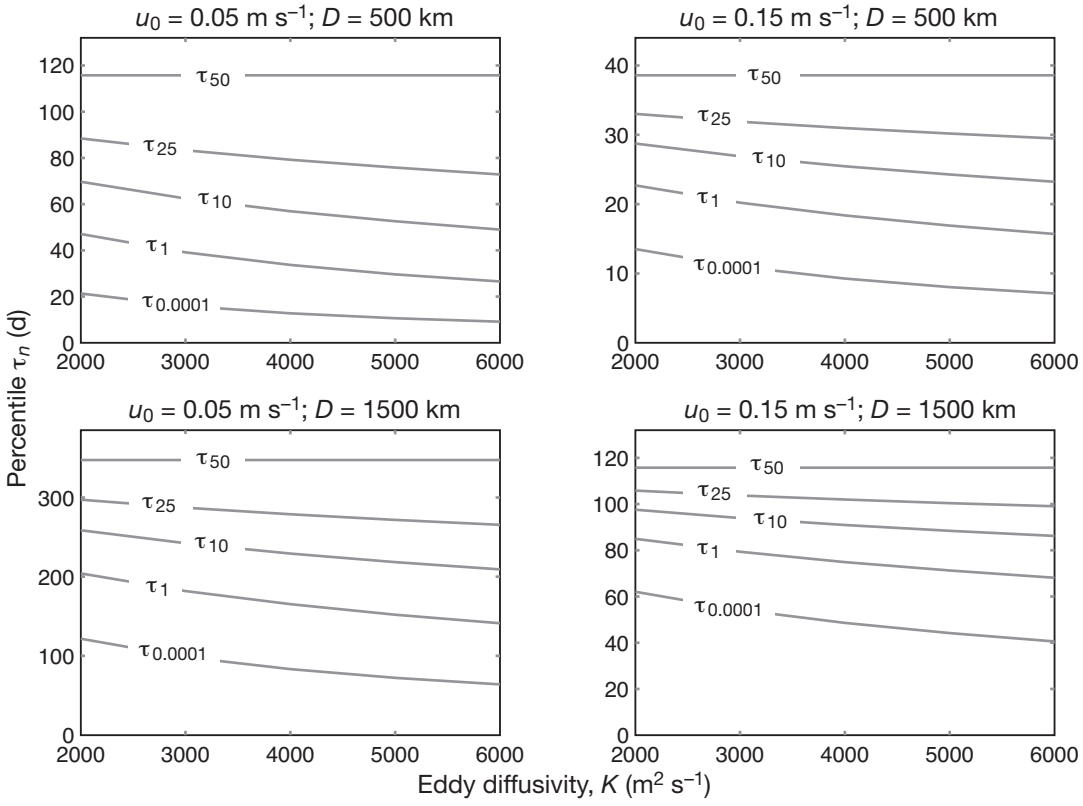

Fig. 6. Temporal kernel percentiles derived from Eq. (12) plotted as a function of eddy diffusivity, K, for 4 hypothetical island pairs

Fig. 6 shows 5 percentiles (τ_{50}, τ_{25}, τ_{10}, $\tau_{0.0001}$) for each combination plotted as a function of eddy diffusivity. For any given mean velocity and separation, the median dispersal time, τ_{50}, is independent of K, but, otherwise, the percentiles decrease in time with increasing K, reflecting the increased spread of the temporal kernel as the ocean eddy diffusivity increases. The lower the percentile, the more the relative change with increasing K. For example, for the slowest ocean with shortest separation (u_0 = 0.05 m s^{-1}, D = 500 km), $\tau_{0.0001}$ ranges from 21 d at K = 2000 m^2 s^{-1} to 9 d at K = 6000 m^2 s^{-1}. If this uncertainty is expressed as a percentage about the mean value, $\tau_{0.0001}$ has an uncertainty of approximately 50%, whereas, for the same example, τ_{10} has an uncertainty of ~20%. Percentiles >50th percentile are not shown here, but will increase with increasing K, and similarly show greater uncertainty for percentiles nearer the tail of the distribution.

As the mean speed or separation increases, the uncertainty in the percentiles becomes less. For the fastest ocean and longest separation (u_0 = 0.15 m s^{-1}, D = 1500 km), $\tau_{0.0001}$ has an uncertainty of ~20% and the uncertainty in τ_{10} drops to ~5%. For some applications, an uncertainty of 50% in an estimate of a relevant percentile may render the calculation impracticable. In other cases, an error of 5% may well be less than the uncertainty in larval duration.

DISCUSSION

One-dimensional advection–diffusion models in which the complexity of ocean physics is parameterised in terms of a few parameters (in this case 2, u_0 and K) are clearly simplifications of the real ocean and are often developed for pedagogical reasons. However, as Largier (2003) notes, this kind of 1-dimensional simplification '[is] reasonably represented by the west coast of the USA … [and] allows development of concepts that can be used also in understanding and quantifying dispersion in more complex configurations'. For these reasons, 1-dimensional random-walk simulations in which ocean physics are contained in 1 eddy diffusivity (or equivalent) parameter are common.

The solutions for the spatial kernel under a Gaussian random-walk model are exact and have appeared in one form or another in the literature. The exact solutions for the temporal kernel presented here are not too difficult to calculate and, in most cases, are how the temporal kernel would be computed. However, for

completeness, we have presented in Supplement 1 approximate solutions for the means and standard deviations of the temporal kernel. These solutions underestimate the true mean and standard deviation with errors that depend on ocean statistics and population separation (Fig. S1 in the supplement at www.int-res.com/articles/suppl/b012p205_supp.pdf).

The solutions for the temporal kernel have been parameterised in terms of the mean velocity and eddy diffusivity. Of these, the eddy diffusivity is likely to have the largest uncertainty. Not only is it difficult to measure K, but, as Okubo (1994) notes, the eddy diffusivity is often regarded as increasing with the length scale of the problem of concern, and there can be differences of several orders of magnitude between the values of K determined for the open ocean compared to that for coastal environments. For example, the values used for illustration in this article ($K \sim 3 \times 10^3$ m^2 s^{-1}) are typical of the open ocean (Zhurbas & Oh 2004), whereas coastal observations of K can be as low as ~100 m^2 s^{-1} (Largier 2003, Chiswell & Stevens 2010). Thus, it is critical to use a value for the eddy diffusivity that is appropriate to the scale of the connectivity problem of interest. While determining an accurate value for K may be one of the most difficult parts of estimating connectivity, we note that this problem is not limited to the random-walk approach, since numerical models also may need tuning to a pre-determined value of eddy diffusivity (Chiswell 2009).

At this point, it is worthwhile commenting on the practical applications of temporal kernels. As well as depending on whether the connection of interest is evolutionary or ecological, the minimum percentile will depend on actual recruitment at the destination population, and is thus related to the total number of larvae that survive the passage. For example, Fig. 5 shows that while Campbell to Chatham Islands has a temporal kernel similar to that for Auckland to Chatham Islands, the number of arrivals was less by nearly an order of magnitude. Thus, all other things being equal (same larval production at Auckland and Campbell Islands, same mortality en route, etc.), any minimum percentile for Campbell to Chatham Islands should be an order of magnitude higher than that for Auckland to Chatham Islands.

One should also recognise that larvae are likely to have a competency period spanning several days (or even months), and the probability of connection during this competency period can be determined from the percentiles corresponding to the upper and lower limits of the competency period. For example, one can compare connectivity from Campbell to Antipodes Islands, for New Zealand sea urchins *Evechinus chloroticus* (larval competency: ~30 to 60 d; Walker 1984) with *Cellana strigilis* (3 to 10 d). The *E. chloroticus* competency limits (60 and 30 d) are the 40 and 1 percentiles of the temporal kernel (Fig. 5), so that, for this species, approximately 39% of all dispersal times would coincide with the competency period. In contrast, only 3×10^{-16}% of dispersal times would coincide with the competency period of the limpet *C. strigilis*. One would conclude that, all other things being equal, the likelihood of urchin dispersal between Campbell and Antipodes Islands is high, whereas that for limpets is near zero.

In reality, it is unlikely that all things are equal. Larval production is highly unlikely to be the same at all sources for all species because of variable breeding-stock and fecundity rates. Mortality will be highly variable and can be crucial in determining connectivity. Chiswell et al. (2003) suggest that larval connection occurs between Australia and New Zealand for *Jasus edwardsii*, but not for *Sagmariasus verreauxi*, despite approximately similar dispersal percentile times, because the former occur to the south in the Tasman Sea where production (and hence available prey) is high, whereas the latter occur farther to the north where there is little production. The implication is that high mortality limits the connection for *S. verreauxi*.

Thus, it becomes virtually impossible to generalise about how to determine the degree to which isolated populations are connected from the temporal kernels. We simply note that these kernels provide tools to estimate connectivity, and that the minimum percentiles will depend on the question of interest. If the Chiswell (2009) results are at all typical, we suggest that evolutionary connectivity may occur for larval durations as low as the 10^{-4} percentile within an order of magnitude. If Cowen & Sponaugle's (2009) estimate of 'several orders of magnitude larger' can be taken literally, then the relevant minimum percentile for ecological connectivity may be around the 1st percentile. These percentiles are low, and illustrate that even ecological connectivity may be controlled by infrequent events, with the consequence that populations can be connected even when the mean dispersal time is many times greater than the larval duration. What is clear is that the mean dispersal time (which can generally be estimated reasonably easily for many population pairs) is not in itself a good indicator of connectivity.

It should, perhaps, be noted that these difficulties also apply when trying to estimate connectivity from spatial kernels, whether derived from simulations or statistical considerations. Not only are the spatial kernels also sensitive to choices in the eddy diffusivity, but one has to make similar decisions, based on numbers of arrivals and larval/gene flow requirements, to decide which percentile of the spatial kernel constitutes connectivity.

Finally, we make the point that temporal kernels will only be inverse Gaussian to the extent that the spatial

kernels are Gaussian. The real ocean is almost certainly more complicated than can be described by simple stochastic models (whether 1- or 2-dimensional), for example, due to inhomogeneous flow, especially in regions of complicated topography. In particular, spatial variability in the time-varying part of the flow can lead to spatial kernels that may also be skewed (e.g. Aiken et al. 2007). However, if the spatial kernel and its time evolution is known, one can use the procedure shown in Fig. 2 to compute the temporal kernel—one replaces $g_n\sigma_n$ in Eq. (7) with a term appropriate to the spatial kernel under consideration. The resulting equations may have to be solved numerically, so that there may be no analytic expressions relating the percentiles to the ocean statistics, but, in principle, the numeric solution can be used just as the analytic solutions proposed here.

Acknowledgements. I thank Graham Rickard for stimulating discussion, and Andy Mckenzie for pointing me to the first-passage solutions. Three anonymous reviewers made comments that contributed to substantial improvement of this article. This work was funded by the Foundation for Research, Science and Technology, New Zealand, Contract No. C01X0223.

LITERATURE CITED

Aiken CM, Navarrete SA, Castillo MI, Castilla JC (2007) Along-shore larval dispersal kernels in a numerical ocean model of the central Chilean coast. Mar Ecol Prog Ser 339:13–24

Babiano A, Basdevant C, Le Roy P, Sadourny R (1987) Single-particle dispersion, Lagrangian structure function and Lagrangian energy spectrum in two-dimensional incompressible turbulence. J Mar Res 45:107–131

Chiswell SM (2009) Colonisation and connectivity by intertidal limpets among New Zealand, Chatham and Sub-Antarctic Islands. II. Oceanographic connections. Mar Ecol Prog Ser 388:121–135

Chiswell SM, Stevens CL (2010) Lagrangian and Eulerian estimates of circulation in the lee of Kapiti Island, New Zealand. Cont Shelf Res 30:515–532

Chiswell SM, Wilkin J, Booth JD, Stanton B (2003) Trans-Tasman Sea larval transport: Is Australia a source for New Zealand rock lobsters? Mar Ecol Prog Ser 247:173–182

Chiswell SM, Rickard GJ, Bowen MM (2007) Eulerian and Lagrangian eddy statistics of the Tasman Sea and southwest Pacific Ocean. J Geophys Res 112:C10004 doi: 10.1029/20070C004110

Cowen RK, Sponaugle S (2009) Larval dispersal and marine population connectivity. Annu Rev Mar Sci 1:443–466

Creese RG (1981) Patterns of growth, longevity and recruitment of intertidal limpets in New South Wales. J Exp Mar Biol Ecol 51:145–171

Folks JL, Chhikara RS (1978) The inverse Gaussian distribution and its statistical application—a review. J R Stat Soc, B 40:263–289

Fratantoni DM (2001) North Atlantic surface circulation during the 1990s observed with satellite-tracked drifters. J Geophys Res 106:22067–22093

Kinlan BP, Gaines SD, Lester SE (2005) Propagule dispersal and the scales of marine community process. Divers Distrib 11:139–148

Largier JL (2003) Considerations in estimating larval dispersal distances from oceanographic data. Ecol Appl 13:71–89

Mace GM, Lande R (1991) Assessing extinction threats: toward a reevaluation of IUCN threatened species categories. Conserv Biol 5:148–157

Mills LS, Allendorf FW (1996) The one-migrant-per-generation rule in conservation and management. Conserv Biol 10:1509–1518

Okubo A (1994) The role of diffusion and related physical processes in dispersal and recruitment of marine populations. In: Sammarco PW, Heron ML (eds) The bio-physics of marine larval dispersal. American Geophysical Union, Washington, DC

Rasmussen LL, Cornuelle BD, Levin LA, Largier JL, DiLorenzo E (2009) Effects of small-scale features and local wind forcing on tracer dispersion and estimates of population connectivity in a regional scale circulation model. J Geophys Res 114:C01012 doi:10.1029/2008JC 004777

Rupolo V (2007) Observing turbulence regimes and Lagrangian dispersal properties in the oceans. In: Griffin DA, Kirwin AD, Mariano AJ, Ozgokmen TM, Rossby R (eds) Lagrangian analysis and prediction of coastal and ocean dynamics. Cambridge University Press, Cambridge

Scheltema RS (1971) Larval dispersal as a means of genetic exchange between geographically separated populations of shallow-water benthic marine gastropods. Biol Bull 140: 284–322

Schrödinger E (1915) Zur Theorie der Fall- und Steigversuche an Teilchen mit brownscher Bewegung. Phys Z 16:289–295

Siegel DA (2003) Lagrangian descriptions of marine larval dispersion. Mar Ecol Prog Ser 260:83–96

Treml EA, Halpin PN, Urban DL, Pratson LF (2008) Modeling population connectivity by ocean currents, a graph-theoretic approach for marine conservation. Landscape Ecol 23:19–36

Walker MM (1984) Larval life span, larval settlement, and early growth of *Evechinus chloroticus* (Valenciennes). N Z J Mar Freshw Res 18:393–397

Zhurbas V, Oh IS (2003) Lateral diffusivity and Lagrangian scales in the Pacific Ocean as derived from drifter data. J Geophys Res 108:3141 doi:10.1029/2002JC001596

Zhurbas V, Oh IS (2004) Drifter-derived maps of lateral diffusivity in the Pacific and Atlantic Oceans in relation to surface circulation patterns. J Geophys Res 109:C05015 doi: 10.1029/2003JC002241

Editorial responsibility: Hans Heinrich Janssen, Oldendorf/Luhe, Germany

Submitted: March 8, 2010; Accepted: February 18, 2011
Proofs received from author(s): May 4, 2011